Supporting Information: Capabilities of asymmetric flow field-flow fractionation coupled to multi-angle light scattering to detect carbon nanotubes in soot in soil

Alexander Gogos[a,c] Ralf Kaegi[b], Renato Zenobi[c], and Thomas D. Bucheli,[a]*

[a]Agroscope, Institute for Sustainability Sciences ISS, 8046 Zurich, Switzerland

[b] Eawag, Swiss Federal Institute of Aquatic Science and Technology, Ueberlandstrasse 133, CH-8600 Duebendorf, Switzerland

[c]Department of Chemistry and Applied Biosciences, ETH Zurich, CH-8093 Zurich, Switzerland

* Corresponding author. Tel.: +41 58 468 73 42; fax: +41 58 468 72 01; e-mail: thomas.bucheli@agroscope.admin.ch.

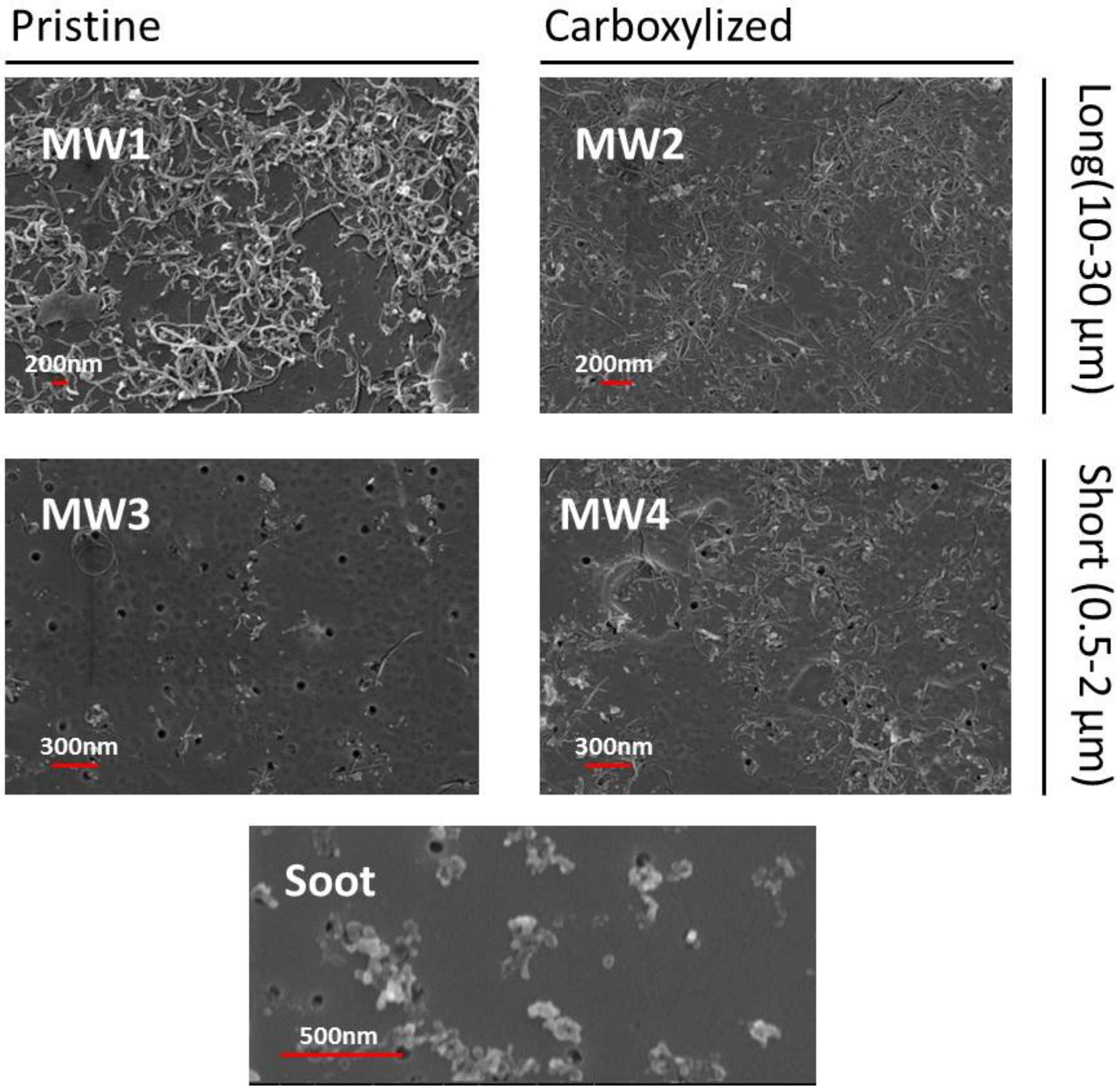

Fig. S1: Example SEM images of the used Soot/MWCNTs suspended in 2%SDC/0.05% NaN_3.

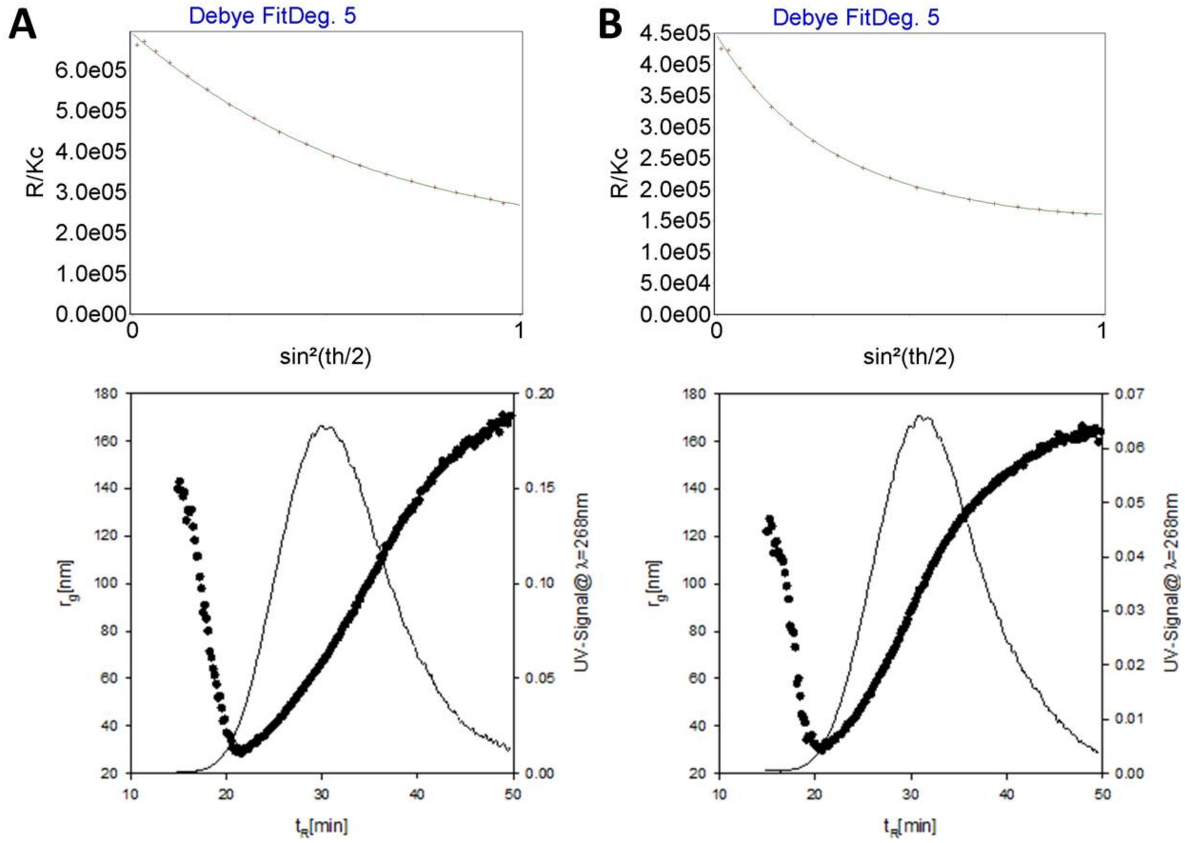

Fig. S2: Example Debye fits (5[th] degree) at maximum peak height for (A) soot and (B) MW1 in pure suspensions. Corresponding r_g (filled circles) distributions and MALS 92° signals (solid lines) are shown below the fits.

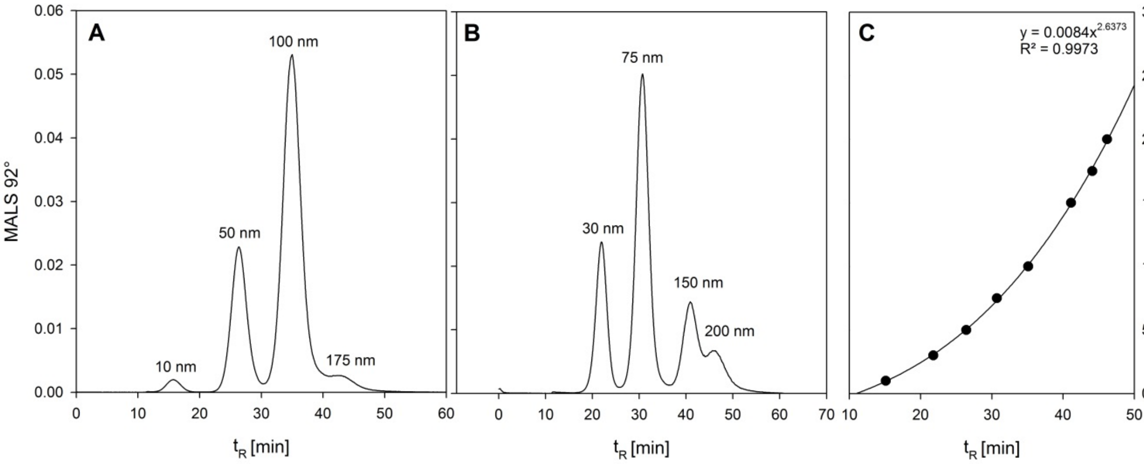

Fig. S3: Example fractograms of the two different mixtures of Nanosphere™ size standards (A and B), as well as the resulting calibration function used to determine r_h (C).

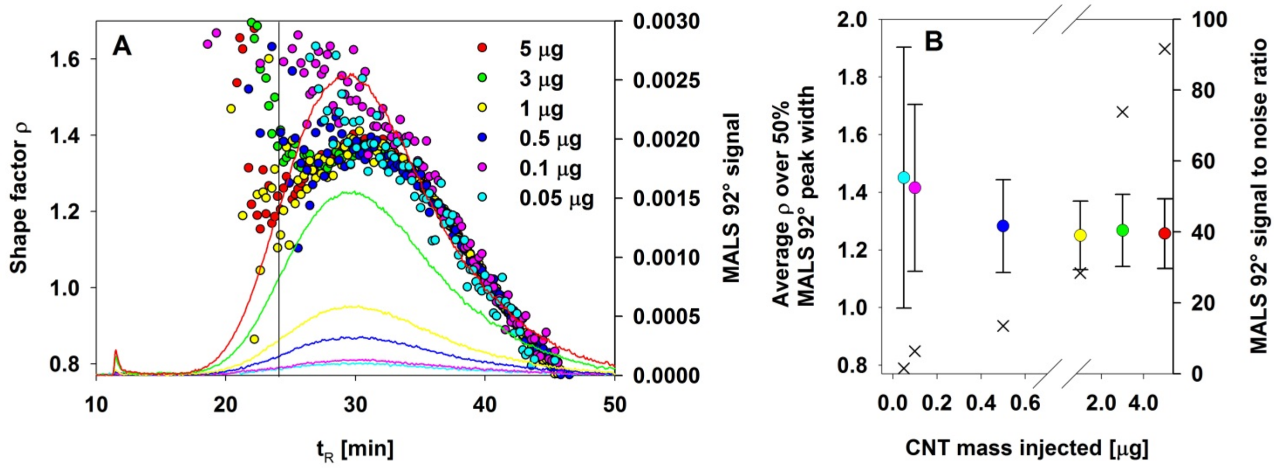

Fig. S4: (A)Fractograms obtained by aF4-MALS with shape factor ρ (colored circles) for different injected masses of MW1. Solid lines represent the MALS 92° signal in the respective color. Vertical line indicates the average transition point between void/steric and normal mode elution. (B) Average shape factor ρ obtained from 50% of the MALS 92° peak width (colored circles) and its signal to noise ratio (crosses) in relation to the injected MW1 mass. Bars represent the standard deviation of the ρ-values over the selected retention time window.

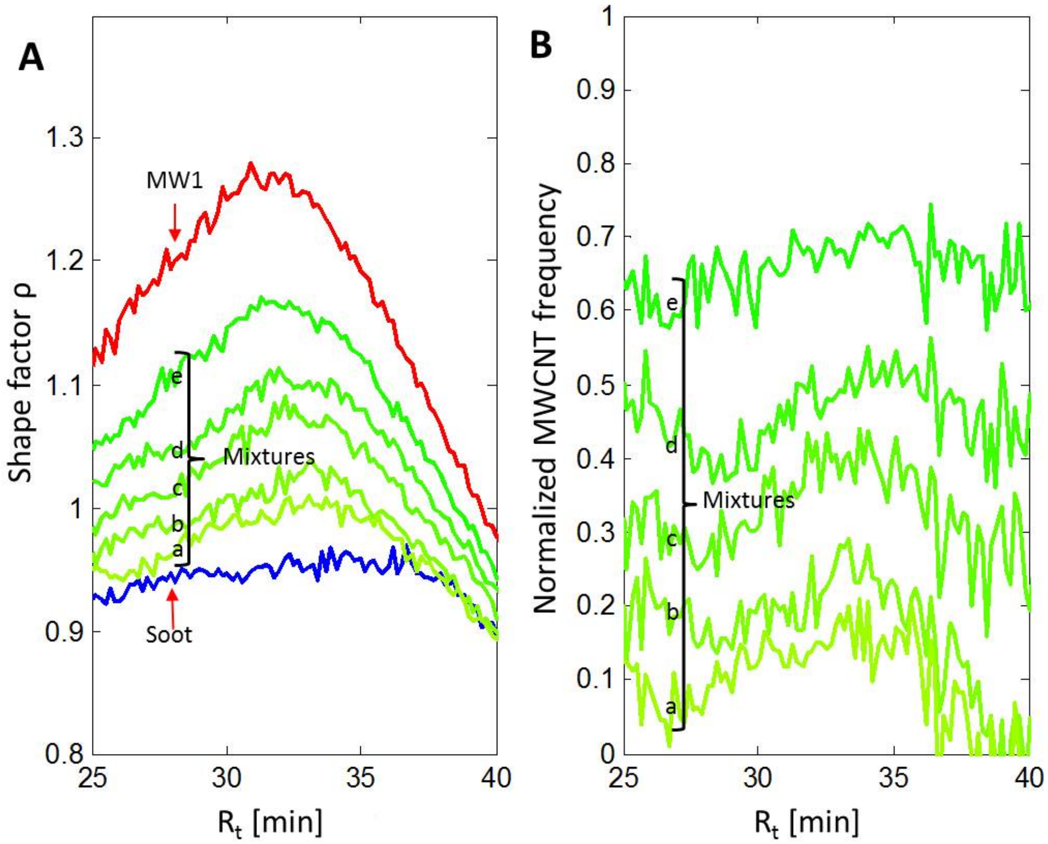

Fig. S5: (A) Fractograms obtained by aF4-MALS with shape factor ρ (lines) of MW1, soot and different mixtures (a-e) of both corresponding to Figure 2 in the main manuscript. (B) Normalized MWCNT-frequency in the five analyzed mixtures of MW1 and soot over the retention time. MWCNT frequencies were calculated in MatLab, comparing ρ-values of the different mixtures at the individual time points relative to the pure MWCNTs.

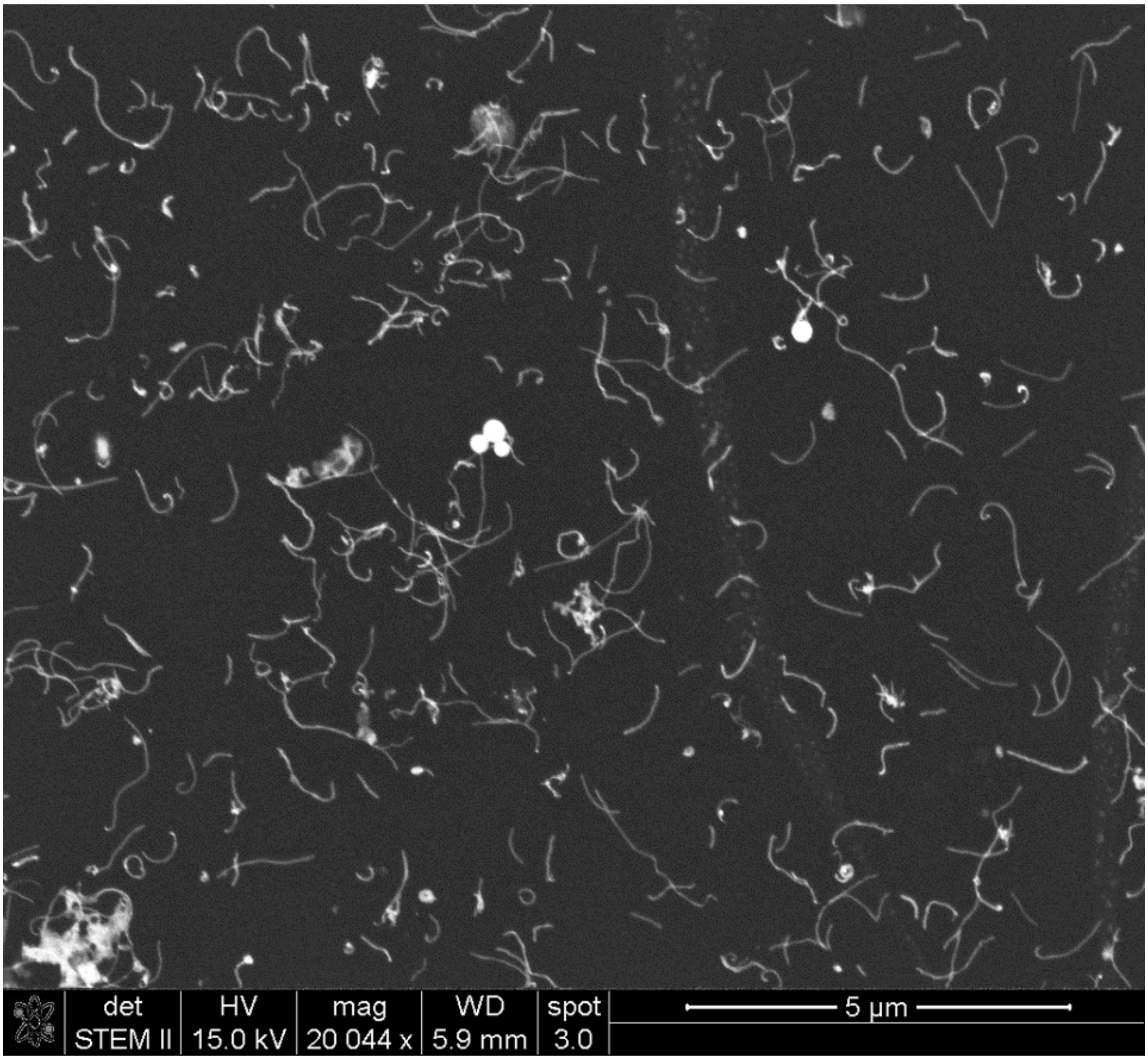

Fig. S6: Example SEM image (transmission mode) of MW1 suspended in 2% SDC/0.05% NaN_3 before fractionation. Note that lengths >1µm are present.

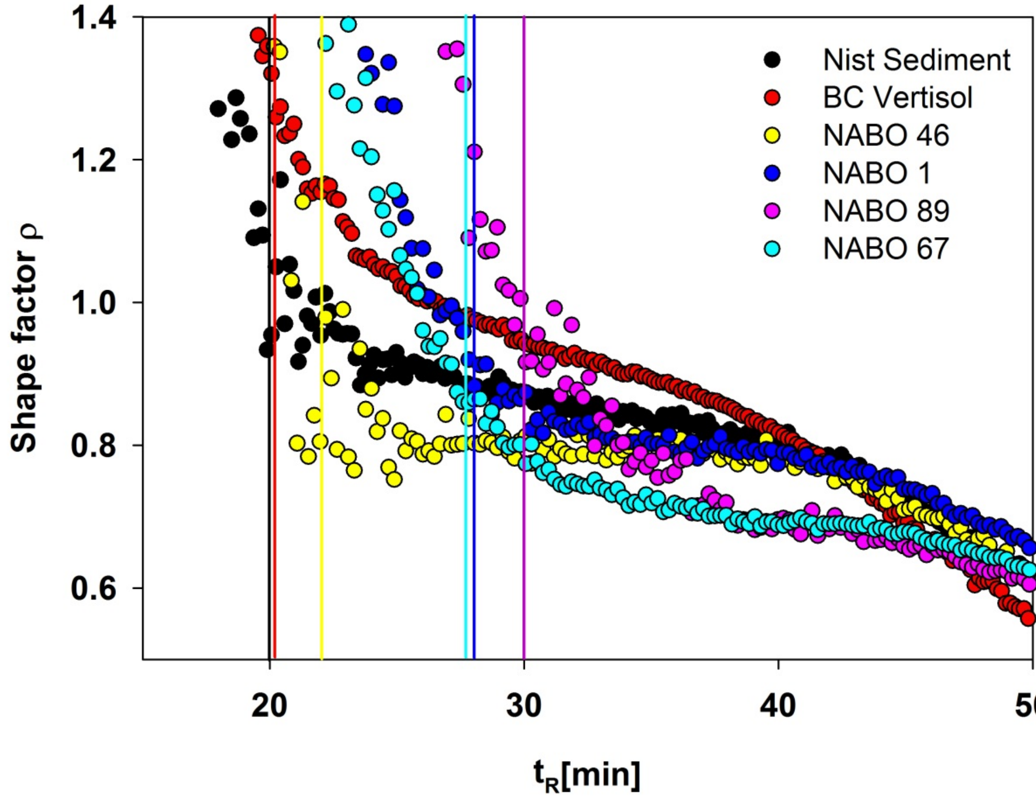

Fig. S7: Fractograms obtained by aF4-MALS with shape factor ρ (symbols) for different soils and a sediment. Values represent the average of three independent measurements. Vertical lines indicate the transition point between void/steric and normal mode elution of the respective soil (colors).

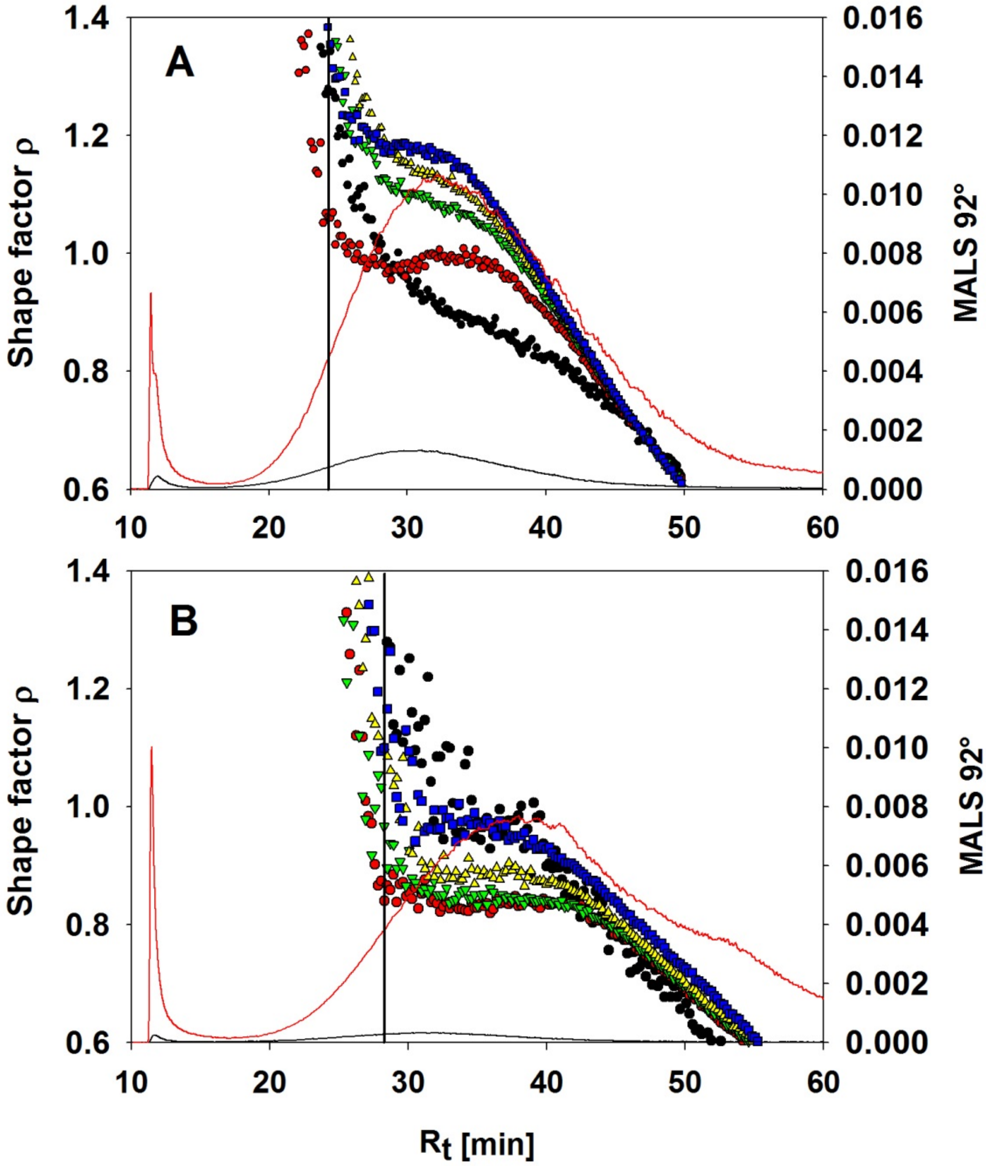

Fig. S8: Fractograms obtained by aF4-MALS with shape factor ρ (symbols) of standard additions of MW1 (A, average values, n=3) and soot (B, n=1) to a Lufa 2.2 soil extract with the following analyte concentrations: 0 (●), 5 (●), 12.5 (▼), 25 (▲), and 50 (■) µg mL^{-1} (corresponding to 1.6, 4, 8.4 and 16.4 mg g-1 of soil, respectively). Vertical line indicates the transition point between void/steric and normal mode elution and solid lines show the 92° MALS signal of the Lufa 2.2 soil extract (black) and the highest concentration of MW1 (A,red) and soot (B, red).

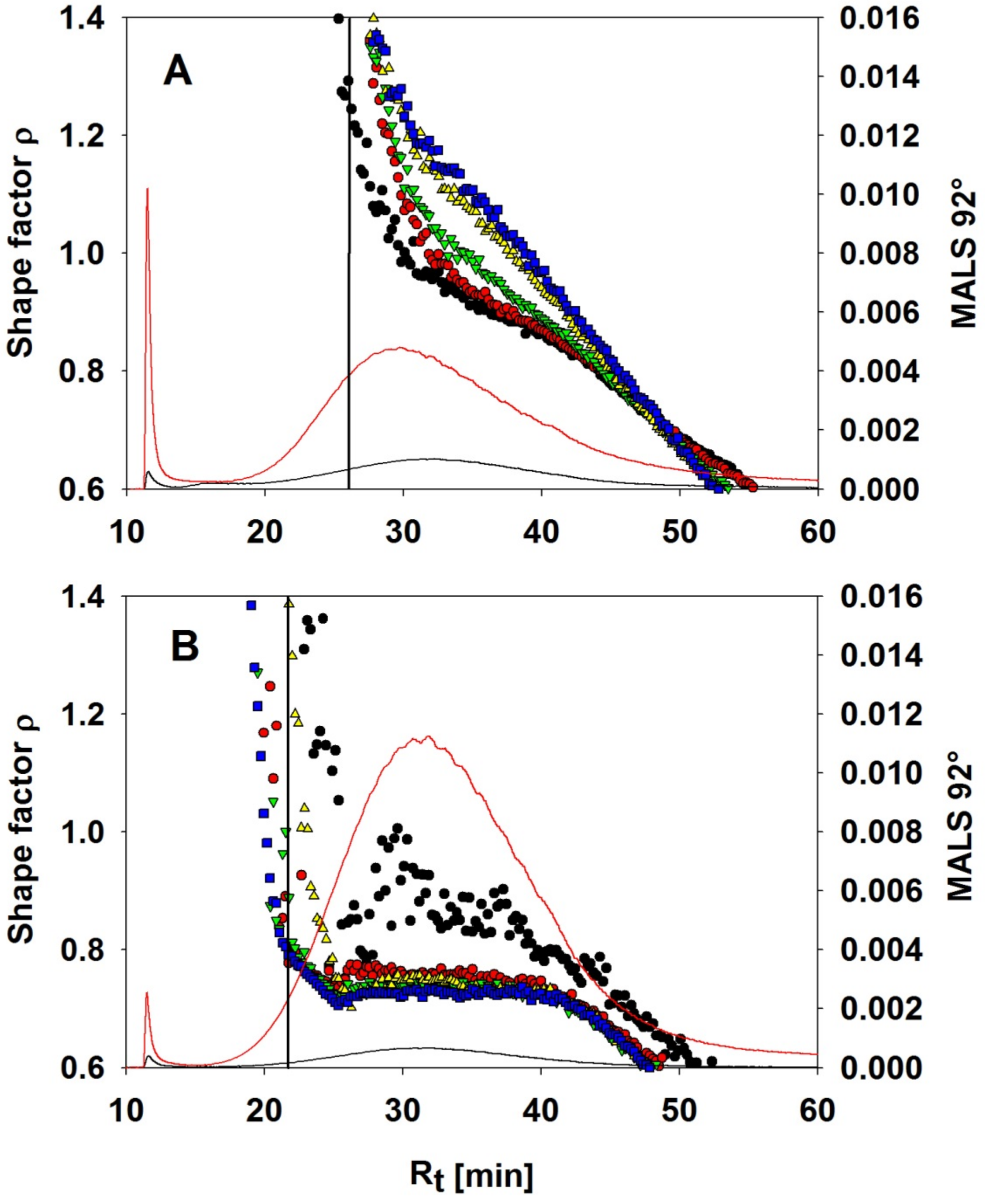

Fig. S9: Fractograms obtained by aF4-MALS with shape factor ρ (symbols) of standard additions of MW1 (A, average values, n=3) and soot (B, n=1) directly to soil with the following analyte concentrations: 0 (●), 1.6 (●), 4 (▼), 8.4 (▲), and 16.4 (■) mg g^{-1}. Vertical line indicates the transition point between void/steric and normal mode elution and solid lines show the 92° MALS signal of the Lufa 2.2 soil extract (black) and the highest concentration of MW1 (A,red) and soot (B, red).

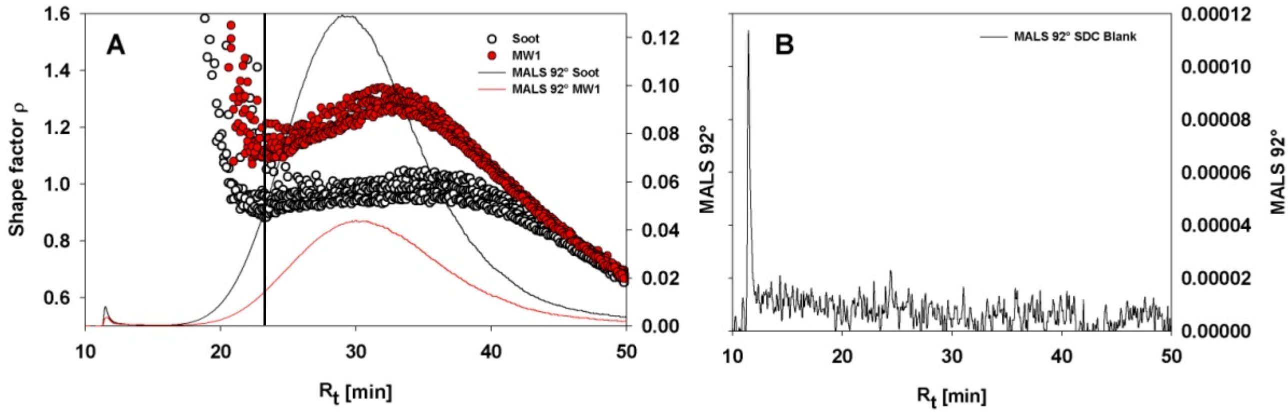

Fig. S10: (A) Alternating injections of Soot and MW1 on the same membrane. Vertical line indicates the transition point between void and normal mode elution. (B) Typical fractograms of the blank 2% SDC/0.05% NaN3 solution used for dispersion of the samples.

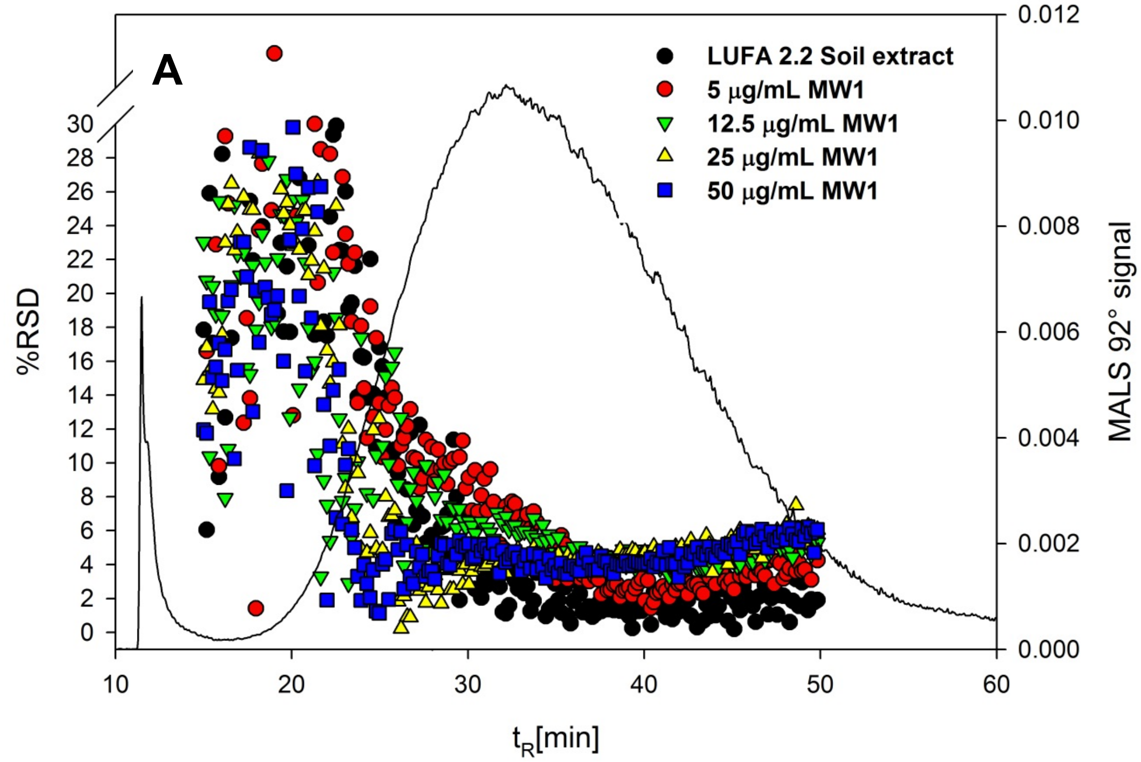

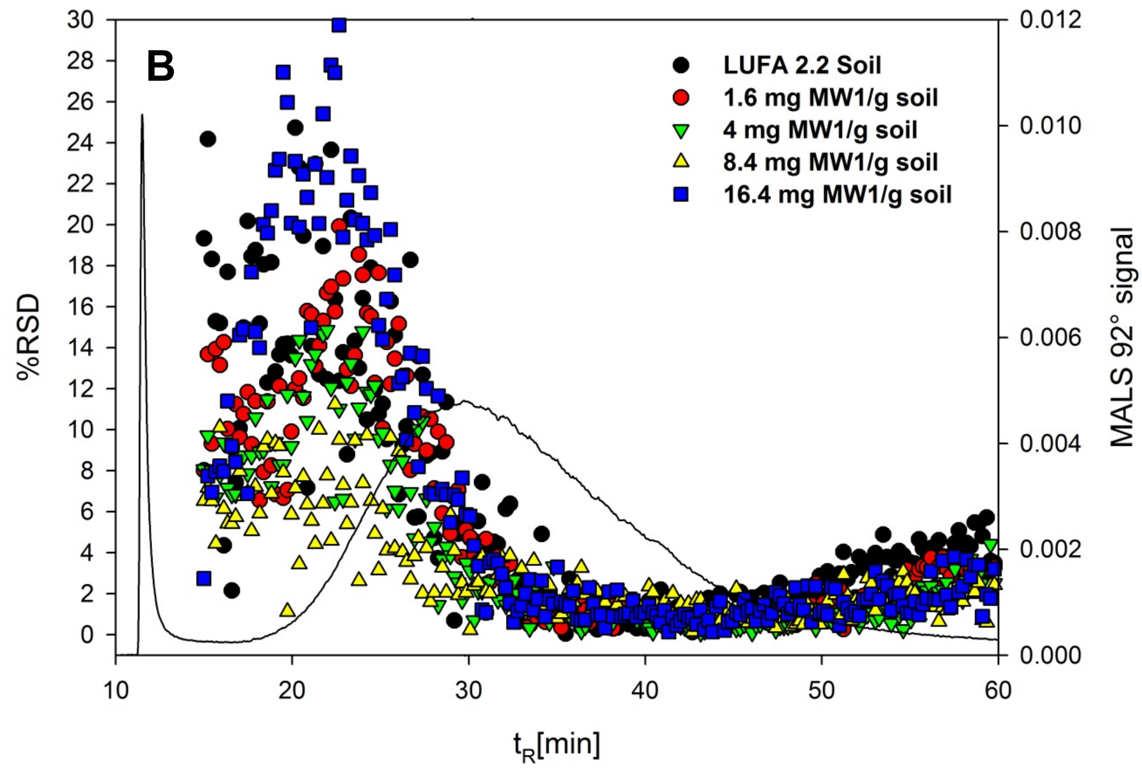

Fig. S11: Relative standard deviations (%RSD) of n=3 independent repeated ρ-measurements of standard additions to a Lufa soil extract (A) and directly to soil (B) (corresponding to article Fig. 4 A and 5 A, respectively). Vertical lines indicate the transition point between void/steric and normal mode elution.

Example for the integration of aF4-MALS into a different analytical workflow: CTO-375

For further illustration, we also analyzed extracts obtained from soil treated by CTO-375 which is often used to isolate BC (Fig. S12† A and B; for information on the procedure also see Sobek and Bucheli[1]). When the native BC content is very low (as in the case of the Lufa 2.2 soil) it can be expected that no difference in ρ between the four MWCNT concentrations applied here is observed after CTO treatment of the soil, because they will be far above the BC concentration anyway (plateau effect, see above). This was confirmed in Fig. S12†A, where unmodified MW1 was spiked to an extract of CTO-375 treated soil. Observed ρ-values in the peak center were comparable to pure MWCNTs. However, when MW1 underwent the complete CTO-375 procedure in soil, some difference in ρ between the concentrations were observed again (Fig. S12†B). During CTO-375, the CNTs are subjected to different oxidizing conditions that may influence their chemical (e.g., surface functionalization) as well as the physical properties (e.g., defects, length)[1]. Thus, to thoroughly combine aF4-MALS with CTO-375, additional knowledge on the transformations that CNTs undergo during the CTO process and their effects on CNT behavior in aF4 is required and could be the objective of future research.

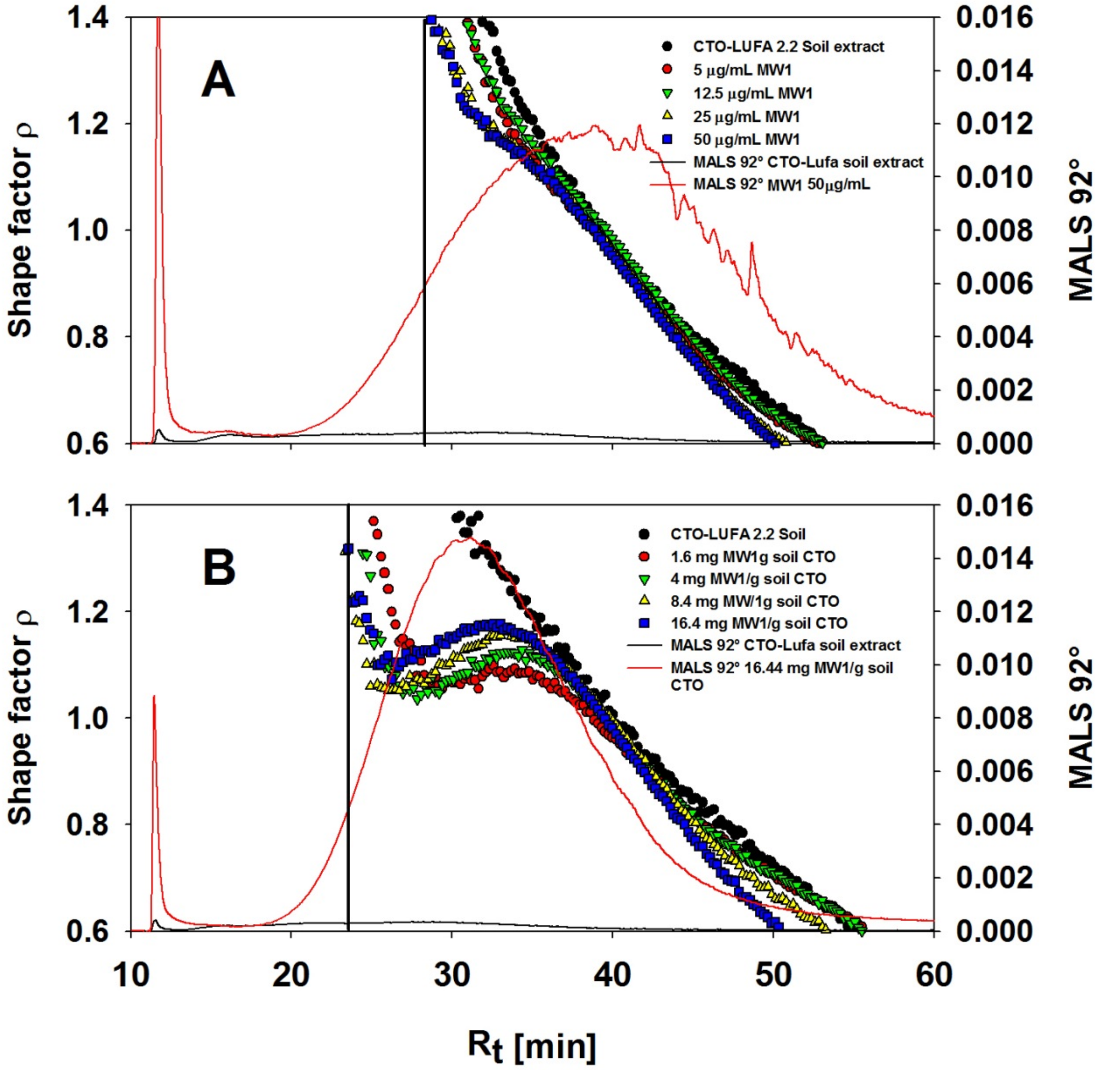

Fig. S12: Fractograms obtained by aF4-MALS with shape factor ρ (symbols) for (A) standard additions of MW1 to an extract of a CTO treated soil and (B) extracts of a MW1-spiked soil treated with CTO-375 (for details see materials and methods section). Values represent the average of three independent replicate measurements. Vertical lines signify the transition point between void/steric and normal mode elution and solid lines the 92° MALS signal of the soil (black) and the highest MW1 concentration (red).

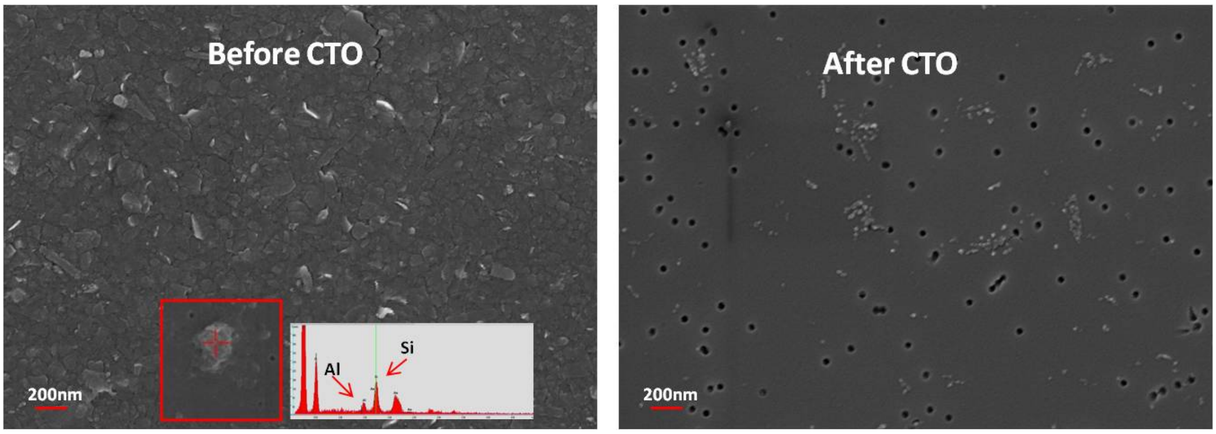

Fig. S13: Example SEM images of Lufa 2.2 soil extracts before and after CTO. Before CTO, mostly organic material is visible, but also some Al-Silicates, as shown below (Measured using EDX). After CTO, extracts are mainly clean.

Table S1: Properties of the carbon nanotubes used in the experiments[1].

MWCNT	Nominal TOC (g/kg dw)	Length (µm)	OD (nm)	ID (nm)	Max. aspect ratio (nominal)	Functionalization (wt%)	SSA (m2/g)	BC 375 °C (g/kg)
MW1	983.5	10-30	20-30	5-10	1500	Pristine	>110	658±28
MW2	974.6	10-30	≤8	2-5	3750	3.86% COOH	>500	567±0.5
MW3	974.6	0.5-2	≤8	3-5	250	Pristine	>500	239±20
MW4	974.9	0.5-2	≤8	3-5	250	4-5% COOH	>500	715±5.3

Table S2: Properties of the used soils.

Soil name	Type	TOC [mg/g]	BC [mg/g]
LUFA 2.2	Loamy sand, agricultural soil	10.0±2[a]	0.2 (n=1)[b]
NIST SRM 1941b	Marine sediment	31.8±3.5[c]	5.1±1.2[d]
BC Vertisol	Clay vertisol	30.6±1.8[c]	1.0±0[c] (0.8±0.5[d])
NABO 1	Clayey loam, grassland soil	38[e]	2.1±0.2[f]
NABO 46	Loamy clay,agricultural soil	28[e]	1.3±0.04[f]
NABO 67	Organic, vegetable gardening	261[e]	11.6±1.5[f]
NABO 89	Organic, Turf	366[e]	4.2±0.3[f]

a)as provided by the distributor, b)this work, c)Ref. [1], d)Ref. [2], e)Ref. [3], f)Ref.[4]

Table S3: %Recovery over different membrane types for MW1 and soot. Values for regenerated cellulose are average of three independent measurements. Other membrane materials have been determined only once (last of three subsequent injections).

Membrane	MW1	Soot
Regenerated Cellulose (RC) 10kDa (n=3)	50	50
Polyvinylidenfluoride (PVDF) 30kDa (n=1)	55	45
Polyethersulfone (PES) 10kDA (n=1)	81	32
Cellulose triacetate (CTA) 10kDa (n=1)	n.d.	n.d.

Literature cited:

1. A. Sobek and T. D. Bucheli, *Environ. Pollut.*, 2009, 157, 1065-1071.
2. K. Hammes, M. W. I. Schmidt, R. J. Smernik, L. A. Currie, W. P. Ball, T. H. Nguyen, P. Louchouarn, S. Houel, Ö. Gustafsson, M. Elmquist, G. Cornelissen, J. O. Skjemstad, C. A. Masiello, J. Song, P. a. Peng, S. Mitra, J. C. Dunn, P. G. Hatcher, W. C. Hockaday, D. M. Smith, C. Hartkopf-Fröder, A. Böhmer, B. Lüer, B. J. Huebert, W. Amelung, S. Brodowski, L. Huang, W. Zhang, P. M. Gschwend, D. X. Flores-Cervantes, C. Largeau, J.-N. Rouzaud, C. Rumpel, G. Guggenberger, K. Kaiser, A. Rodionov, F. J. Gonzalez-Vila, J. A. Gonzalez-Perez, J. M. de la Rosa, D. A. C. Manning, E. López-Capél and L. Ding, *Global Biogeochem. Cycl.*, 2007, 21, GB3016.
3. BUWAL, *Nationales Bodenbeobachtungsnetz: Messresultate 1985-1991*.
4. T. Agarwal and T. D. Bucheli, *Environ. Pollut.*, 2011, 159, 532-538.